Soft Matter

Dynamic Article Links

Cite this: *Soft Matter*, 2012, **8**, 11708

www.rsc.org/softmatter

PAPER

Density anomaly in a fluid of softly repulsive particles embedded in a spherical surface

Santi Prestipino, Cristina Speranza and Paolo V. Giaquinta*

Received 24th July 2012, Accepted 10th September 2012
DOI: 10.1039/c2sm26706c

We investigated the volumetric anomaly of a two-dimensional system of particles embedded in the surface of an inert sphere. The interaction between particles was modeled with a purely repulsive Gaussian potential. The phase diagram of the model exhibits one single fluid phase since the absence of an attractive term in the potential rules out a liquid–vapour phase transition while the curved geometry inhibits the formation of a long-range-ordered crystalline arrangement. Nonetheless, we found that the thermodynamic behavior of the model is, in some aspects, qualitatively reminiscent of that observed in a much more complex liquid such as supercooled water confined in cylindrical silica nanopores. In fact, upon cooling the fluid isobarically, the number density exhibits – over a range of moderately low pressures – a two-fold anomaly: a maximum followed, at lower temperatures, by a shallow minimum. Interestingly, a minimum also shows up in the density of the two-dimensional triangular solid which, for similar values of pressure and temperature, is the stable phase in a flat space. The two loci, traced by the thermodynamic parameters for which the density attains its minimum value in the fluid and in the solid phase, run very close to each other, a behavior which suggests that the emergence of the density minimum is not affected by the nature of the stable host phase but is more basically rooted in the properties of the interatomic potential.

I. Introduction

The list of "anomalous" properties of water currently includes up to sixty-eight entries.[1] Among these, the most famous one certainly is the negative thermal expansivity that is manifested by water on approaching the freezing point, over a temperature range whose upper boundary corresponds to the temperature of maximum density (TMD). The observation of this behavior at ambient pressure dates back to the very origins of modern experimental science.[2] One might then wonder whether, upon cautiously cooling water so as to avoid it to congeal, this substance should eventually re-enter, even though as a metastable liquid, a "normal" volumetric regime characterized by a positive thermal expansivity. The corresponding threshold would then coincide with a minimum of the density as a function of temperature.

To the best of our knowledge, the first, though problematic, indication of the existence of such a minimum in metastable bulk water was given a century ago by P. W. Bridgman.[3] His pioneering investigations of the effects of pressure on the temperature dependence of the molar volume showed that a density minimum should actually be expected on physical grounds, even though its observation at a given pressure might be effectively impeded by the supervening termination of the accessible metastable region. In more recent years, Angell and coworkers, while discussing the properties of water in relation with other tetrahedral liquids,[4] also argued that the overall volumetric behavior of such systems does, of necessity, imply the existence of a density minimum, but also emphasized that observing it in a laboratory experiment may be a rather difficult task.

The first theoretical confirmations of the plausibility of the thermodynamic scenario originally envisaged by Bridgman eventually came from an accurate molecular theory which accounts in a simple way for the effects of geometric constraints on hydrogen bonding.[5] This theory predicts that the density minimum is present in the deeply supercooled bulk liquid and moves to higher temperatures upon confinement between two parallel hydrophobic walls.[6] Unambiguous evidence of a density minimum later emerged from numerical simulation studies of various rigid-molecule potential models of bulk liquid water[7–9] as well as, more recently, from an efficient Monte Carlo simulation of a coarse-grained model of a water monolayer within hydrophobic walls.[10] In this latter study the anomaly has been associated with the rearrangement of the hydrogen-bond network in the low-temperature sub-diffusive regime.

On the experimental side, the first indication of a density minimum in deeply supercooled water was obtained in water confined, at normal pressure, within silica nanopores.[11,12] The estimated temperature of minimum density (TmD) was about 210 K. However, there is no general consensus so far on whether

Università degli Studi di Messina, Dipartimento di Fisica, Contrada Papardo, 98166 Messina, Italy. E-mail: santi.prestipino@unime.it; cristina.speranza@unime.it; paolo.giaquinta@unime.it

the observed feature can be considered a property of the "bulk", albeit metastable, liquid or, rather, an effect produced by the confinement of water on a nanometer scale.

Based on the above evidence, a view has developed that the density minimum may actually be a genuine property of supercooled water which, as yet, has not been observed at ambient pressure just because its emergence is preempted by the vanishing of the ice-nucleation barrier at about 230 K. A different explanation is apparently suggested by the data of Erko and coworkers for nanoconfined water;[13] in fact, these authors observed the rough merging, on cooling, of the confined-system and bulk-solid density branches for temperatures lower than TmD. This behaviour suggests that water in the nanopore core has, to all probabilities, transformed into ice. Since solidification is washed out as a sharp transition, nanoconfinement would effectively manage to bridge the gap between the liquid and solid density branches, thus giving rise to a density minimum. We finally recall that, aside from water, the minimum-density anomaly has been observed in tellurium,[14] also mixed with sulphur.[15]

While awaiting the experimental confirmation of the existence of the density minimum in water at higher than ambient pressures, one may try to learn something more from simplified models that still retain the gist of the water system. In this respect, the minimum-density anomaly has been detected even in rather archetypal one-dimensional (1D) model fluids.[16,17] Indeed, it is well known that particles interacting through isotropic core-softened potentials display many water-like anomalies, including a density maximum in the fluid phase.[18,19] The simplest system of this kind is probably the Gaussian-core model (GCM),[20–22] in which the bounded interparticle repulsion has a Gaussian shape. However, as yet no minimum-density anomaly has been observed in the fluid phase of the GCM, neither in three nor in two dimensions.[23] Somewhat surprisingly, this feature was found instead in one dimension,[24] where no fluid–solid transition occurs in a strict thermodynamic sense. On this basis, one might speculate that the density minimum appears whenever the hosting space is such that the solid is suppressed as a proper thermodynamic phase. In order to verify this guess, we simulated the behavior of the GCM system on a sphere. Spherical boundary conditions (SBC) do actually prevent an extended and defect-free triangular network of bonds from being established, this way pushing the stability range of the fluid phase to virtually zero temperature. In such a setting, the melting transition of the planar GCM reduces to a crossover phenomenon. The trick of curving space so as to induce the frustration of crystalline order has also been used as a means to tune the slowing down of the relaxation processes associated with glass formation.[25]

Simulating Gaussian repulsive particles embedded in a spherical surface, far from being only an interesting conceptual exercise, may actually provide useful information on the behavior of real molecular substances under locally inhomogeneous conditions such as those that are typically found in the first hydration shell of a globular protein. It is not unreasonable to imagine that, using a suitable local probe, one might succeed in disentangling the properties of solvation water from those pertaining to the hydrated protein.[26] Alternatively, it should be possible to measure, within an atomistic simulation of one single protein immersed in a water bath maintained at constant pressure, the density of solvated water, thus allowing the thermodynamic behavior investigated here to be checked in a more realistic system. In this regard, we recall that protein hydration water is known to exhibit, similarly to bulk water, a dynamic fragile-to-strong glass crossover at low temperatures;[27,28] hence, it may reasonably be expected that other bulk-water anomalies are shared by solvation water.

The outline of this paper is as follows. In Section II we illustrate the model and the simulation method. The results are then presented in Section III, together with a discussion of their potential relevance for an understanding of the minimum-density anomaly in water. Some concluding remarks are finally given in Section IV.

II. Model and method

We investigated a classical system of particles interacting through the repulsive potential $u(r) = \varepsilon \exp(-r^2/\sigma^2)$, where r is the interparticle distance while ε and σ are the energy and length scaling constants, respectively. In a flat 2D space the GCM system exhibits, below a maximum melting temperature, a reentrant melting transition, *i.e.*, the melting of the solid upon isothermal compression. As a result, the fluid phase is thermodynamically stable at low and high pressures. The reentrant melting transition turns out to be continuous and occurs in two stages, through an intermediate hexatic phase.[23] When particles are located on a sphere, the melting transition gets blurred and ceases to be a thermodynamic singularity, turning into a crossover phenomenon.[29,30] Note that in a spherical geometry the distance r corresponds to the length of the shortest arc joining two particles: $r = R \arccos(\boldsymbol{R}_1 \cdot \boldsymbol{R}_2/R^2)$, where $\boldsymbol{R}_1$ and $\boldsymbol{R}_2$ are the vector radii of the particles and R is the sphere radius.

We simulated the GCM system in the isothermal–isobaric ensemble, using the Metropolis Monte Carlo (MC) method with SBC. For selected values of the pressure P we ran, starting from a state at relatively high temperature, a sequence of MC simulations, advancing with steps $\Delta T^* = -0.0005$, where $T^* = k_B T/\varepsilon$ is the reduced temperature. Correspondingly, the reduced density and pressure are defined as $\rho^* = \rho\sigma^2$ and $P^* = P\sigma^2/\varepsilon$.

At each state point the system was equilibrated for a long time (one to two million sweeps, one sweep corresponding to N trial MC moves), before generating an equilibrium trajectory of, typically, two million sweeps. We investigated systems with sizes $N = 200$ and $N = 500$, since spherical boundary conditions introduce a stronger N dependence of thermodynamic and structural properties than in the flat space under periodic boundary conditions.

Besides the particle number density ρ and the average energy per particle E/N, we computed the specific heat at constant pressure, $C_P = T(\partial s/\partial T)_P$, where s is the entropy per particle, the isothermal compressibility, $K_T = -v^{-1}(\partial v/\partial P)_T$, where $v = \rho^{-1}$ is the average volume per particle, and the thermal expansion coefficient, $\alpha_P = v^{-1}(\partial v/\partial T)_P$. We also calculated the orientational correlation function (OCF) $h_6(r)$, whose definition is the same as given in ref. 29, namely

$$h_6(r) = \langle \cos\{6[\theta(\boldsymbol{R}_1) - \theta(\boldsymbol{R}_2)]\} \rangle, \quad (1)$$

where r is the spherical distance between the particles whose positions are defined by $\boldsymbol{R}_1$ and $\boldsymbol{R}_2$, and $\theta(\boldsymbol{R}_1)$ is the angle, measured on the plane tangent to the sphere at $\boldsymbol{R}_1$, between the

arc joining the particle at $\boldsymbol{R}_1$ with a nearest neighbor (chosen at random among those identified through the Voronoi construction) and the direction pointing from $\boldsymbol{R}_1$ to $\boldsymbol{R}_2$.

III. Simulation results

The curvature of the sphere imposes an excess of five-fold over seven-fold coordinated particles,[30] thus preventing the formation of extended crystallites. As a result, the system is in a disordered phase at any density and down to very low temperatures. We note, however, that the lower the temperature the more difficult is simulating the system at equilibrium, since it becomes eventually trapped in a local energy minimum, with the result that the relaxation to equilibrium does not occur in a reasonable simulation time. A typical snapshot of the system with 500 particles at low temperature and moderate pressure is reported in Fig. 1. We see a pervasive triangular particle network that is punctuated with chain-like defects most of which are 5-7-5 trimers.

Following the procedure described in the previous section, we investigated the phase behavior of the GCM fluid on a sphere in a range of moderate to large reduced pressures (0.3–2.0) and for reduced temperatures lower than 0.03. As expected, neither the number density nor the energy exhibits any (even rounded-off) jump discontinuity in the explored domain. However, while the energy is a smooth increasing function of the temperature for all pressures, the density shows a more complex behavior. In Fig. 2 we plotted the number density as a function of the temperature for various pressures. We clearly see the emergence of both a minimum and a maximum in a narrow pressure range ($0.35 \lesssim P^* \lesssim 0.45$, for $N = 500$); for larger pressures, only the maximum survives. A magnification of this behavior is presented in Fig. 3 for three values of the pressure and for both explored sizes. While a maximum in the density of the GCM fluid had already been observed in three[31] as well as in two dimensions,[23] the emergence of a shallow minimum in the density of a 2D system is, to our knowledge, a novel finding.

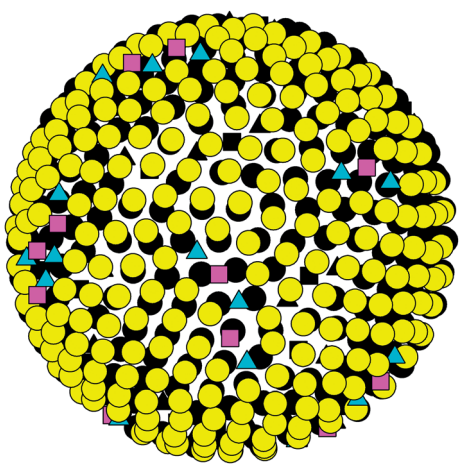

Fig. 1 A snapshot of the system taken for $P^* = 0.38$ and $T^* = 0.005$. Particles are represented as circles whose diameter has been arbitrarily set equal to σ. Open circles: sixfold coordinated particles (front side of the spherical surface); triangles: fivefold coordinated particles; squares: sevenfold coordinated particles; solid black symbols: particles located on the back side of the spherical surface.

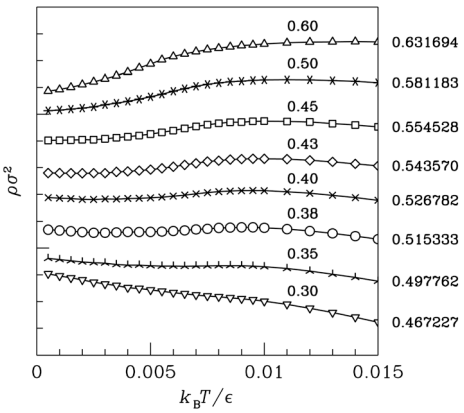

Fig. 2 Reduced number density plotted as a function of the reduced temperature for increasing pressures in the range $0.30 \leq P^* \leq 0.60$ (data for 500 particles). The curves were shifted along the vertical direction so as to make their main features more visible; the separation between two major tick marks along the left vertical axis is equal to 0.005, while the absolute scale has been fixed through the value of each curve at $T^* = 0.015$ that is reported on the right vertical axis.

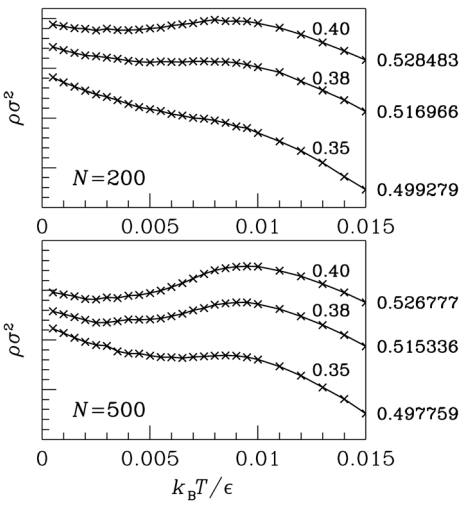

Fig. 3 Reduced number density plotted as a function of the reduced temperature for three values of the reduced pressure ($P^* = 0.35$, 0.38, 0.40) and for two sets of data: $N = 200$, upper panel; $N = 500$, lower panel. The separation between two major tick marks along the left vertical axis is equal to 0.0005, while the absolute scale has been fixed through the value of each curve at $T^* = 0.015$ that is reported on the right vertical axis.

One might legitimately wonder whether the data points relative to the lowest temperatures presented in Fig. 3 are the outcome of well-equilibrated sampling runs or are possibly flawed, thus reflecting a glassy non-ergodic behaviour. Indeed, upon deeply cooling the system at constant pressure, it will eventually enter a dynamic regime characterized by longer and longer equilibration times. One way to settle the controversy would be to follow the particles in their motions throughout the surface, in order to check whether equilibration at a given temperature has actually been achieved or not. Indeed, two possibilities may occur: either the particles get trapped inside self-imposed cages at all times or they keep on diffusing freely on the

sphere. Therefore, for selected values of the reduced temperature in the range $0.001 \leq T^* \leq 0.005$, we computed the average cosine of the angular separation, α, between the current and the initial positions of a particle as a function of the MC time lag, τ. The resulting data were then fitted at long times to the law

$$\langle \cos \alpha(\tau) \rangle = \exp\{-2D\tau/\sigma^2\}, \quad (2)$$

which, as such, applies to a Brownian walker on a rigid sphere.[32] The quantity $\langle \cos \alpha(\tau) \rangle$ has been plotted for various temperatures, at the reduced pressure $P^* = 0.4$, in Fig. 4. We see that, after the initial ballistic behaviour at short times, all the curves show a typical diffusional trend, with no indication of a saturation at long times. Hence, we can safely conclude that the system dynamics is effectively ergodic down to the lowest sampled temperatures, though for $T^* \leq 0.002$ particles diffuse so slowly that their average shift after 2×10^6 sweeps is at most of the order of σ. In the light of the results of ref. 29 and 30, we expect that at such extremely low temperatures point defects are clustered in well-separated regions, which remain frozen for long times, thus causing a global suppression of self-diffusion. Upon cooling the system, the total number of disclinations gradually drops, more rapidly across the melting line of the planar system, until it levels off at about 4% of the particle number in the pressure range where the density shows a minimum. At low temperatures the difference between the average numbers of five-fold and seven-fold particles is maintained practically equal to 12.[30]

The volumetric anomaly gives rise to related anomalies in the thermodynamic response functions.[24] In particular, a minimum in α_P and a maximum in C_P show up along an isobaric path (see Fig. 5 and 6). As for the isothermal compressibility, we found that, for reduced pressures in the range $1 < P^* < 2$, its rate of change as a function of the temperature is so small that the maximum which would be expected on account of the thermodynamic arguments illustrated in ref. 24 is so weak a feature that it is likely buried in the statistical noise of the data.

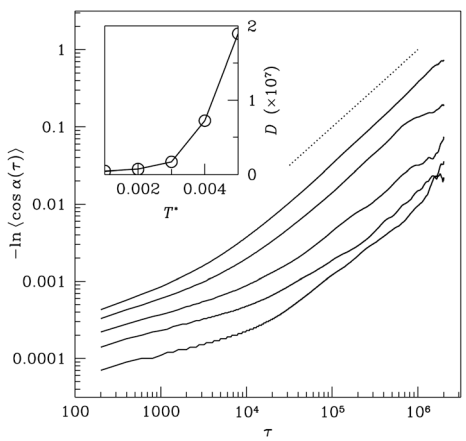

Fig. 4 Log–log plot of $Y(\tau) \equiv -\ln\langle\cos\alpha(\tau)\rangle$ (see text) for $P^* = 0.4$ and for a number of temperatures (from top to bottom, $T^* = 0.005$, 0.004, 0.003, 0.002, 0.001). $Y(\tau)$ may be viewed as the analogue, for a particle confined to a spherical surface, of the mean square displacement (MSD) of a particle on a plane (τ is the time lag measured in sweeps; the data have been collected during a production run of 2×10^6 sweeps). The dotted straight line with unit slope was plotted for the reader's convenience. The shorter τ the larger is the statistical accuracy of the datum; this explains why the spherical MSD gets more irregular for the largest τ values shown. Inset: $D(T)$ in units of σ^2 per sweep as obtained through a linear fit of the Y data in the range $4.5 \leq \log \tau \leq 6$.

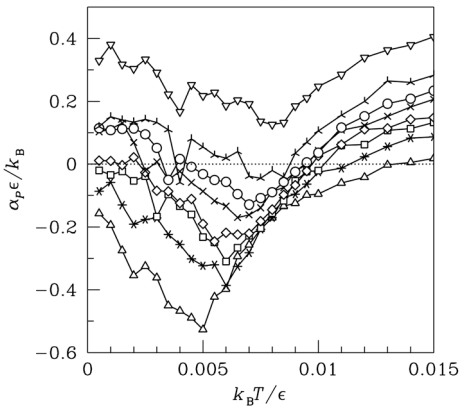

Fig. 5 Thermal expansion coefficient plotted as a function of the reduced temperature for different reduced pressures (data for 500 particles): inverted triangles, $P^* = 0.30$; tripods, $P^* = 0.35$; circles, $P^* = 0.38$; crosses, $P^* = 0.40$; diamonds, $P^* = 0.43$; open squares, $P^* = 0.45$; stars, $P^* = 0.50$; triangles, $P^* = 0.60$.

The loci in the P–T plane corresponding to an extremum of either the density or of a thermodynamic response function are depicted in Fig. 7. The overall morphology of all such lines is analogous to that found in the 1D GCM fluid.[24] Thus, the temperature loci corresponding to the isobaric minimum of the thermal expansivity and to the isobaric maximum of the specific heat run very close to each other and, as expected, cross the boundary of the density-anomaly region (*i.e.*, the region where $\alpha_P < 0$) at the point of confluence of the TMD and TmD lines.

The volumetric behavior of the GCM fluid in a spherical geometry can also be contrasted with that of the planar 2D system, which shares an identical local structure. While no special feature besides the density maximum has been observed all along the metastable fluid branch of the planar GCM, we found instead that the number density of the triangular solid

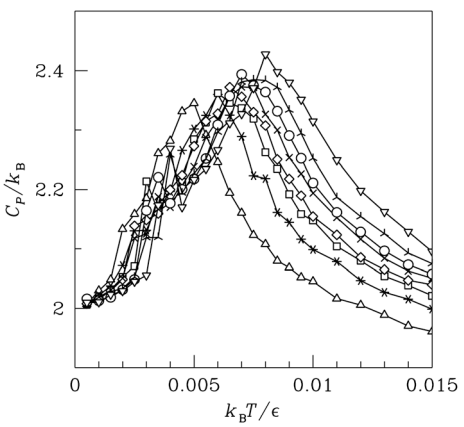

Fig. 6 Isobaric specific heat plotted as a function of the reduced temperature for different reduced pressures (data for 500 particles); same notation as in Fig. 5. Though visual inspection is hampered by the partially overlapping datasets plotted in the figure, the monotonic evolution of the maximum with pressure is clear.

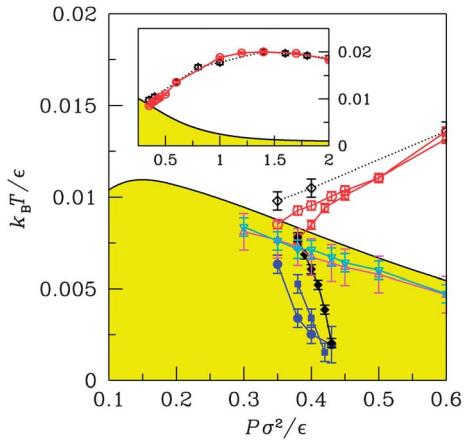

Fig. 7 Location of the density and thermodynamic response functions extrema in the P–T plane (we used polynomial interpolations to locate maxima and minima). Black line: melting line of the planar GCM system (the solid phase is stable at lower temperatures); open circles: temperatures of maximum density (TMD) for $N = 500$; open squares: TMD line for $N = 200$; open diamonds: TMD line of a planar GCM fluid; solid circles: temperatures of minimum density (TmD) for $N = 500$; solid squares: TmD line for $N = 200$; solid diamonds: TmD line of the planar GCM solid; open triangles: temperatures of minimum thermal expansivity; open inverted triangles: temperatures of maximum isobaric specific heat. The inset shows the TMD lines for $N = 500$ and for the planar GCM fluid, plotted over a more extended pressure range. Lines traced through the data points are a guide to the eye.

exhibits a minimum in a narrow pressure interval: $0.38 \leq P^* \leq 0.43$ (see Fig. 8). The data refer to MC simulations carried out on a system of 1152 particles. The locus of such minima, when plotted on the P–T plane, is seen to run very close to the density-minima locus of the spherical GCM fluid. This manifest correspondence suggests that the emergence of the density minimum

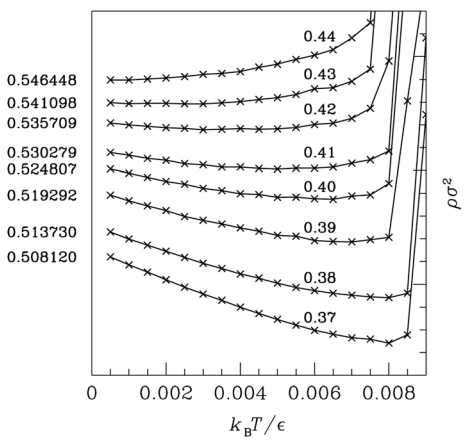

Fig. 8 Reduced number density of the planar GCM solid plotted as a function of the reduced temperature with increasing pressures over the range $0.37 \leq P^* \leq 0.44$. The data were obtained upon simulating a system with $N = 1152$ particles. All curves were shifted along the vertical direction so as to make their features more clearly visible; the separation between two major tick marks along the left vertical axis is equal to 0.0005, while the absolute scale has been fixed through the value of each curve at $T^* = 0.0005$ that is reported on the left vertical axis.

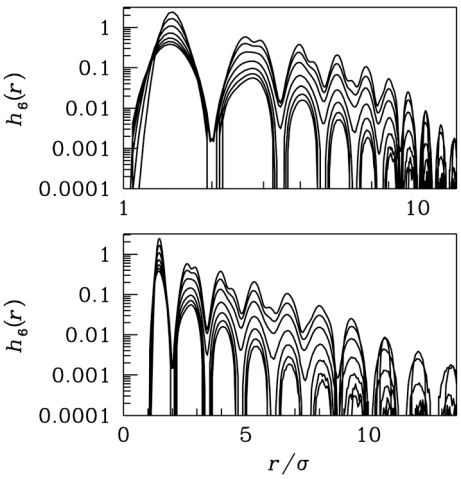

Fig. 9 Orientational correlation function (OCF) for a system of 500 particles at the reduced pressure $P^* = 0.4$. The reduced temperature varies from 0.015 down to 0.003 with steps of −0.002 (lower curves refer to higher temperatures). Top panel: log–log plot; bottom panel: log–lin plot. The OCF was plotted only up to $r/\sigma = 13.6$, which roughly corresponds to the distance $\pi R/2$ from a pole to the equator.

in the 2D GCM system is not conditioned by the ordered or disordered nature of the stable host phase but is more basically rooted in the properties of the interatomic potential.

Lastly, we comment on the spatial modulation of the OCF, which is reported in Fig. 9 for $P^* = 0.4$ and reduced temperatures in the range $0.003 \leq T^* \leq 0.015$. For the relatively small size considered here ($N = 500$), looking at the large-distance decay of $h_6(r)$ does not make much sense. A natural upper cutoff for interparticle separations on the sphere is $r_c = \pi R/2$, corresponding to the distance from a pole to the equator. For distances in the range $r_c/2 \leq r \leq r_c$, the decay of the $h_6(r)$ maxima in Fig. 9 is more akin to being exponential rather than algebraic, which suggests that the orientational order in this system remains short-ranged until at least $T^* = 0.003$. Below this temperature, the equilibration of the fluid becomes at best difficult, as can be guessed from the fact that, for $T^* = 0.001$ and 0.002, the profile of $h_6(r)$ at medium and large distances still is highly irregular, notwithstanding a production-run length of more than two million MC sweeps.

IV. Conclusions

In this paper we have studied the equilibrium properties of a system of Gaussian particles embedded in a spherical surface, with a focus on the anomalous behavior of the number density and of the thermodynamic response functions. Under spherical boundary conditions, no extended crystalline order is possible though, at low temperatures, local particle arrangements can hardly be distinguished from those found in the solid. In two dimensions the melting transition becomes blurred, with the effect of extending the thermodynamic stability of the fluid phase down to $T = 0$. Under such conditions, if the system size is not too large, the Gaussian-core model (GCM) is expected to exhibit thermodynamic anomalies that are analogous to those found in

one dimension as well as in metastable water confined inside a nanocylinder.

Indeed, in the phase diagram of the GCM fluid on a sphere we have identified a region of anomalous volumetric behavior ($\alpha_P < 0$) that is bounded at high temperatures by a locus of density maxima and, at low temperatures, by a locus of density minima. Both such lines stem from a common point C, where the first and second temperature derivatives of the density are both zero. We have also identified lines of maximum isobaric specific heat and of minimum thermal-expansion coefficient that cross the boundary of the anomalous-density region at C.

We have ascertained that density minima are also present in the crystalline phase of the flat GCM, while being absent in the fluid phase. Interestingly, the associated density-minima locus runs close, in the P–T plane, to the corresponding locus of the system in a curved geometry, a circumstance which strongly suggests that this feature has its roots in the nature of the GCM interaction potential and in the *local* spatial arrangements that it generates at low temperatures and high pressures.

It would certainly be interesting to verify whether the thermodynamic phenomenology exhibited by a system of Gaussian particles on a sphere can be observed on a layer of solvation water surrounding a globular protein, like lysozyme or myoglobin.

Acknowledgements

The authors acknowledge interesting exchanges of ideas with Prof. Francesco Mallamace.

References

1 See, for instance, the website entitled "*Water structure and science*" maintained by M. Chaplin at http://www.lsbu.ac.uk/water/index2.html.
2 *Saggi di naturali esperienze fatte nell'Accademia del Cimento sotto la protezione del serenissimo principe Leopoldo di Toscana*, Firenze, 1667; See also W. E. K. Middleton, *The Experimenters: A study of the Accademia del Cimento*, The John Opkins Press, Baltimore, 1971.
3 P. W. Bridgman, *Proc. Am. Acad. Arts Sci.*, 1912, **47**, 441.
4 C. A. Angell, R. D. Bressel, M. Hemmati, E. J. Sare and J. C. Tucker, *Phys. Chem. Chem. Phys.*, 2000, **2**, 1559.
5 T. M. Truskett, P. G. Debenedetti, S. Sastry and S. Torquato, *J. Chem. Phys.*, 1999, **111**, 2647.
6 T. M. Truskett, P. G. Debenedetti and S. Torquato, *J. Chem. Phys.*, 2001, **114**, 2401.
7 I. Brovchenko, A. Geiger and A. Oleinikova, *J. Chem. Phys.*, 2003, **118**, 9473; I. Brovchenko, A. Geiger and A. Oleinikova, *J. Chem. Phys.*, 2005, **123**, 044515.
8 P. H. Poole, I. Saika-Voivod and F. Sciortino, *J. Phys.: Condens. Matter*, 2005, **17**, L431.
9 D. Paschek, *Phys. Rev. Lett.*, 2005, **94**, 217802.
10 F. de los Santos and G. Franzese, *J. Phys. Chem. B*, 2011, **115**, 14311.
11 D. Liu, Y. Zhang, C.-C. Chen, C.-Y. Mou, P. H. Poole and S.-H. Chen, *Proc. Natl. Acad. Sci. U. S. A.*, 2007, **104**, 9570.
12 F. Mallamace, C. Branca, M. Broccio, C. Corsaro, C.-Y. Mou and S.-H. Chen, *Proc. Natl. Acad. Sci. U. S. A.*, 2007, **104**, 18387.
13 M. Erko, D. Wallacher, A. Hoell, T. Hauss and O. Paris, *Phys. Chem. Chem. Phys.*, 2012, **14**, 3852.
14 Y. Tsuchiya, *J. Phys.: Condens. Matter*, 1991, **3**, 3163.
15 Y. Tsuchiya, *J. Phys.: Condens. Matter*, 1992, **4**, 4335.
16 M. R. Sadr-Lahijany, A. Scala, S. V. Buldyrev and H. E. Stanley, *Phys. Rev. E: Stat. Phys., Plasmas, Fluids, Relat. Interdiscip. Top.*, 1999, **60**, 6714.
17 A. Ben-Naim, *J. Chem. Phys.*, 2008, **128**, 024505.
18 G. Malescio, F. Saija and S. Prestipino, *J. Chem. Phys.*, 2008, **129**, 241101.
19 See S. V. Buldyrev, G. Malescio, C. A. Angell, N. Giovambattista, S. Prestipino, F. Saija, H. E. Stanley and L. Xu, *J. Phys.: Condens. Matter*, 2009, **21**, 504106, and references therein.
20 F. H. Stillinger, *J. Chem. Phys.*, 1976, **65**, 3968.
21 S. Prestipino, F. Saija and P. V. Giaquinta, *Phys. Rev. E: Stat., Nonlinear, Soft Matter Phys.*, 2005, **71**, 050102(R).
22 P. V. Giaquinta and F. Saija, *ChemPhysChem*, 2005, **6**, 1768.
23 S. Prestipino, F. Saija and P. V. Giaquinta, *Phys. Rev. Lett.*, 2011, **106**, 235701.
24 C. Speranza, S. Prestipino and P. V. Giaquinta, *Mol. Phys.*, 2011, **109**, 3001.
25 F. Sausset, G. Tarjus and P. Viot, *Phys. Rev. Lett.*, 2008, **101**, 155701.
26 F. Mallamace, private communication, (2012).
27 S.-H. Chen, L. Liu, E. Fratini, P. Baglioni, A. Faraone and E. Mamontov, *Proc. Natl. Acad. Sci. U. S. A.*, 2006, **103**, 9012.
28 F. Mallamace, C. Corsaro, P. Baglioni, E. Fratini and S.-H. Chen, *J. Phys.: Condens. Matter*, 2012, **24**, 064103.
29 S. Prestipino Giarritta, M. Ferrario and P. V. Giaquinta, *Phys. A*, 1992, **187**, 456.
30 S. Prestipino Giarritta, M. Ferrario and P. V. Giaquinta, *Phys. A*, 1993, **201**, 649.
31 See *e.g.* P. Mausbach and H.-O. May, *Fluid Phase Equilib.*, 2006, **249**, 17.
32 See *e.g.* J.-M. Caillol, *J. Phys. A: Math. Gen.*, 2004, **37**, 3077.